









Large-Amplitude Oscillatory Motion of Mercury's Cross-Tail Current Sheet

Gangkai Poh^{1,2} , Weijie Sun³ , Kellyn M. Clink³, James A. Slavin³ , Ryan M. Dewey³ , Xianzhe Jia³ , Jim M. Raines³ , Gina A. DiBraccio² , and Jared R. Espley² 

¹Center for Research and Exploration in Space Sciences and Technology II, University of Maryland, Baltimore County, Baltimore, MD, USA, ²Solar System Exploration Division, NASA Goddard Space Flight Center, Greenbelt, MD, USA, ³Department of Climate and Space Sciences and Engineering, University of Michigan, Ann Arbor, MI, USA

Key Points:

- Large-amplitude oscillations of Mercury's cross-tail current sheet (or flapping waves) with period of ~4 – 25 s were observed
- Flapping motion of Mercury's cross-tail current sheet warped and tilted the current sheet in the y - z plane
- Flapping waves preferentially occur in Mercury's duskside current sheet

Correspondence to:

G. Poh,
gangkai.poh@nasa.gov

Citation:

Poh, G., Sun, W., Clink, K. M., Slavin, J. A., Dewey, R. M., Jia, X., et al. (2020). Large-amplitude oscillatory motion of Mercury's cross-tail current sheet. *Journal of Geophysical Research: Space Physics*, 125, e2020JA027783. <https://doi.org/10.1029/2020JA027783>

Received 6 JAN 2020

Accepted 29 MAY 2020

Accepted article online 19 JUN 2020

Abstract We surveyed 4 years of MESSENGER magnetic field data and analyzed intervals with observations of large-amplitude oscillatory motions of Mercury's cross-tail current sheet, or flapping waves, characterized by a decrease in magnetic field intensity and multiple reversals of B_x , oscillating with a period on the order of ~4 – 25 seconds. We performed minimum variance analysis (MVA) on each flapping wave event to determine the current sheet normal. Statistical results showed that the flapping motion of the current sheet caused it to warp and tilt in the y - z plane, which suggests that these flapping waves are kink-type waves propagating in the cross-tail direction of Mercury's magnetotail. The occurrence of flapping waves shows a strong preference in Mercury's duskside plasma sheet. We compared our results with the magnetic double-gradient instability model and examined possible flapping wave excitation mechanism theories from internal (e.g., finite gyroradius effects of planetary sodium ions Na^+ on magnetosonic waves) and external (e.g., solar wind variations and K-H waves) sources.

1. Introduction

Continuous in situ magnetic field and plasma measurements observed by MESSENGER have allowed us to gain insights on the dynamic processes occurring in different regions of Mercury's magnetotail, from the northern and southern tail lobes to the cross-tail current sheet embedded within the central plasma sheet (DiBraccio, Slavin, Raines, et al., 2015; Poh et al., 2017a; Rong et al., 2018; Slavin et al., 2012; Sun et al., 2020). Although the structure and processes occurring in Mercury's magnetotail are known to be qualitatively similar to that of Earth's, they are different in spatial and temporal scale (e.g., Gershman et al., 2014; Poh et al., 2017b; Raines et al., 2011; Sun et al., 2015). Recent simulation studies (Chen et al., 2019; Liu et al., 2019) suggest that kinetic-scale dynamics and instabilities dominate in Mercury's small magnetotail (~10 d_i wide, where d_i is the ion inertial length), thereby explaining the observed asymmetric structure and occurrence of processes in the tail.

The oscillatory (or flapping) motion of Earth's cross-tail current sheet has been extensively studied by various missions, such as THEMIS (Sun et al., 2014) and Cluster (Gao et al., 2018; Rong et al., 2015, 2018; Runov et al., 2005; Sergeev et al., 2003; Sun et al., 2010; Zhang et al., 2002), and is commonly identified in the magnetic field measurements as multiple reversals of the x component of the magnetic field B_x (i.e., multiple crossings of the current sheet) (Speiser & Ness, 1967). Note: The Geocentric Solar Magnetospheric (GSM) coordinate system is commonly used in these Earth studies where the x axis points toward the Sun along the Sun-Earth line, the z axis is the projection of the Earth's dipole axis onto the plane perpendicular to the x axis, and the y axis completes the right-handed system. These statistical studies have shown that such oscillatory motion of Earth's cross-tail current sheet has an average period of ~1–10 minutes and generally propagates as a wave in the dawn-dusk direction from the midnight meridian to the tail flanks at velocities of few tens of km/s. As such, the current sheet is predominantly tilted in the y - z plane during the observations of these flapping waves (Sergeev et al., 2006; Volwerk et al., 2013). Earlier correlation studies further suggested a relationship between the occurrence of flapping waves at Earth and magnetic reconnection-related phenomena such as fast magnetospheric flows (e.g., Davey et al., 2012) and substorm activities (Sergeev et al., 2006). Figure 1 shows an illustration of the kink-type magnetotail oscillations propagating in the dawn-dusk direction (see Rong et al., 2015, for illustrations of flapping waves observed at Earth). For this type of magnetotail flapping motion, the sinusoidal flapping waves propagate in the

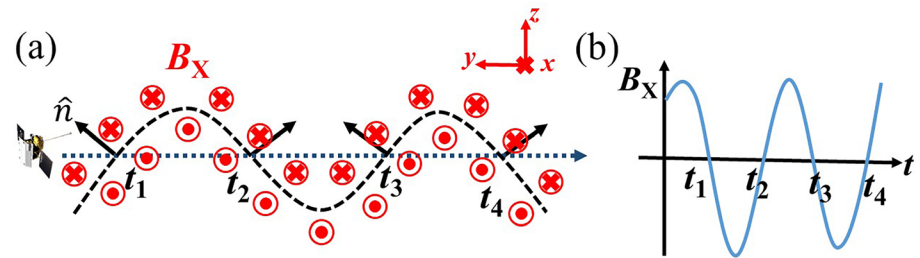


Figure 1. (a) Illustration of kink-type flapping motion of the cross-tail current sheet. The black arrows represent the current sheet normal vector, while the blue arrow represents the direction of the current sheet motion. (b) Expected magnetic field signatures in the MSM x component for kink-type current sheet flapping.

cross-tail direction (blue dashed arrows) with the cross-tail current sheet tilted in the y - z plane (as shown by the “tilted” current sheet normal \mathbf{n}) during each crossing of the center of the current sheet at times t_1 , t_2 , t_3 , and t_4 . Therefore, the current sheet normal vectors between adjacent current sheet crossings are expected to “oscillate” in the y - z plane (i.e., change in the sign of the y component with small x component of the current sheet normal) as shown in Figure 1a; the spacecraft is expected to observe multiple polarity reversals of B_x for this type of magnetotail oscillation mode. Note that the time periods when the spacecraft observed the positive and negative part of the B_x reversal and their respective amplitudes are dependent on the spacecraft trajectory relative to the average location of the center of the sinusoidal current sheet in the frame of the flapping current sheet. We would like to emphasize that the use of directional terms (e.g., dawn-dusk and north-south) in this paper does not represent any specific directionality (i.e., dawn-dusk may represent dawn to dusk or dusk to dawn).

Not unique to Earth, these flapping motions of the cross-tail current sheet are also observed in other intrinsic and induced planetary magnetospheres, such as those of the giant planets (Jupiter and Saturn) (Volwerk et al., 2013), Venus (Rong et al., 2015), Mars (DiBraccio et al., 2017), and Mercury (Poh et al., 2017a, 2017b, 2018). Despite the limited analysis of the flapping waves using only single-spacecraft measurements from most planetary missions, statistical results show that the flapping waves observed in planetary magnetotails are generally similar to those observed at Earth where the flapping current sheets are also tilted in the y - z plane, consistent with the idea that the flapping waves propagate toward or away from the flanks (Volwerk et al., 2013).

A natural follow-up question is: What is the formation mechanism for these current sheet oscillations? Statistical studies at Earth (e.g., Sergeev et al., 2006) suggested that these dawn-dusk propagating waves are most likely to be driven by an internal source within the magnetotail. Based on spacecraft observations, several flapping wave excitation mechanisms, such as the ballooning-type (Golovchanskaya & Maltsev, 2005) and the magnetic double-gradient instability (Duan et al., 2018; Erkaev et al., 2007, 2008, 2009a, 2009b, 2010; Korovinskiy et al., 2016, 2018), have been proposed. Observational studies at Earth (Forsyth et al., 2009; Sun et al., 2014) demonstrated that the magnetic double-gradient instability model best describes the observational data. Other observational (Forsyth et al., 2009; Shen et al., 2008) and numerical (Juusola et al., 2018; Sergeev et al., 2008) studies had also proposed solar wind variations as an external source for the excitation of flapping waves within Earth’s magnetotail.

In this study, we seek to determine the differences and similarities of current sheet flapping in Mercury’s magnetotail, where kinetic-scale instabilities dominate (Chen et al., 2019; Liu et al., 2019), and Earth’s magnetotail, which is well described by MHD. We would like to emphasize that MESSENGER is a single-spacecraft mission. Unfortunately, many of the multispacecraft analysis techniques employed to accurately determine the physical properties (e.g., propagation direction and speed) of these flapping waves are unavailable in our single-spacecraft Mercury study. Therefore, with MESSENGER’s single-spacecraft measurements, we are restricted to the use of the minimum variance analysis (MVA) technique (Sonnerup & Scheible, 1998) to analyze and infer some of the properties of the large-amplitude flapping waves observed at Mercury. The MVA technique had also been successfully applied to many earlier studies using single-point measurements at Earth [e.g., AMPTE/IRM satellite (Sergeev et al., 1998) and Geotail

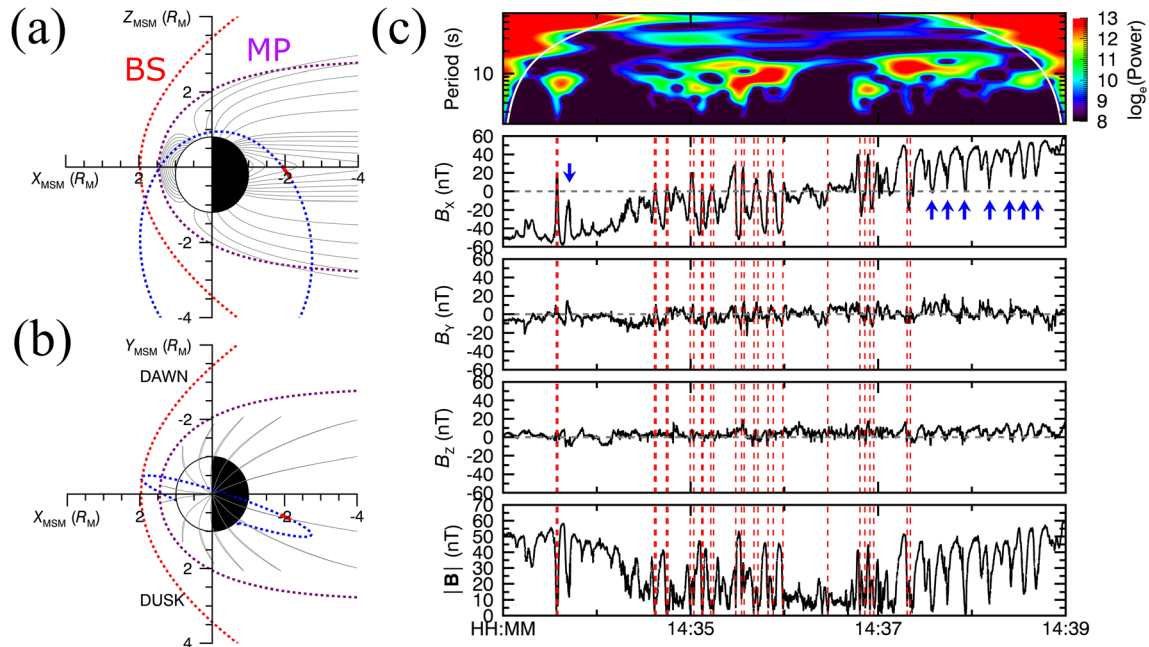


Figure 2. Orbit of MESSENGER on 19 May 2012 in the (a) meridional and (b) equatorial planes. Red and purple dashed lines represent the location of Mercury's model bow shock and magnetopause, respectively (Winslow et al., 2013). Blue dashed line represents MESSENGER's orbit around Mercury on 19 May 2012, and the gray lines show the scaled T96 model magnetic field lines (Tsyganenko, 1995) using a linear scaling factor of 8. (c) Full-resolution magnetic field measurements of MESSENGER encounter of Mercury's cross-tail current sheet on 19 May 2012. Panel 1 shows wavelet analysis of B_x , and panels 2–5 show three components and magnitude of magnetic field measurements, respectively. Dotted red lines and blue arrows represent full and partial flapping wave events, respectively.

(Sergeev et al., 2006)] and other planets [e.g., Galileo and Cassini (Volwerk et al., 2013)]. Our statistical results show that the current sheet oscillations observed in Mercury are similar to those observed at Earth in that Mercury's current sheet during flapping motion is also tilted in the y - z plane, suggesting that the waves propagate in the cross-tail direction. We compared our results with the magnetic double-gradient instability model and examined different internal- and external-source formation theories and models proposed previously.

2. Flapping Waves Event Selection and Data Analysis

In this study, we surveyed the full-resolution 20 vectors per second magnetic field (Anderson et al., 2007) measurements from MESSENGER's Magnetometer (MAG) to identify magnetotail crossings with observations of current sheet flapping wave event. We chose the aberrated Mercury Solar Magnetospheric (MSM') coordinate system for the analyses performed in this study. The Mercury Solar Magnetospheric (MSM) coordinate system is a coordinate system centered on Mercury's internal offset dipole (Anderson et al., 2011) with the positive x axis in the sunward direction (i.e., antiparallel to the solar wind flow) along the Sun-Mercury line, the z axis is positive northward parallel to Mercury's magnetic dipole moment axis, and the y axis completes the right-handed system. A correction for solar wind aberration is then applied to the MSM coordinate system to create the MSM' coordinate system. This correction assumes a radial solar wind speed of 400 km/s and uses Mercury's perpendicular orbital velocity computed daily.

2.1. 19 May 2012 Event

Figure 2 shows an example of MESSENGER's observation of Mercury's magnetotail on 19 May 2012. Figures 2a and 2b show MESSENGER's trajectory through Mercury's magnetotail in the meridional (i.e., x - z) and equatorial (i.e., x - y) planes, respectively. With its polar orbital trajectory, MESSENGER traversed Mercury's duskside magnetotail in the z direction. Figure 2c shows the magnetic field measurements observed by MESSENGER during the traversal. Panel 1 of Figure 2c shows the wavelet analysis (Jenkins & Watts, 1968) of the x component of the observed magnetic field, while Panels 2–5 show the x , y , and z

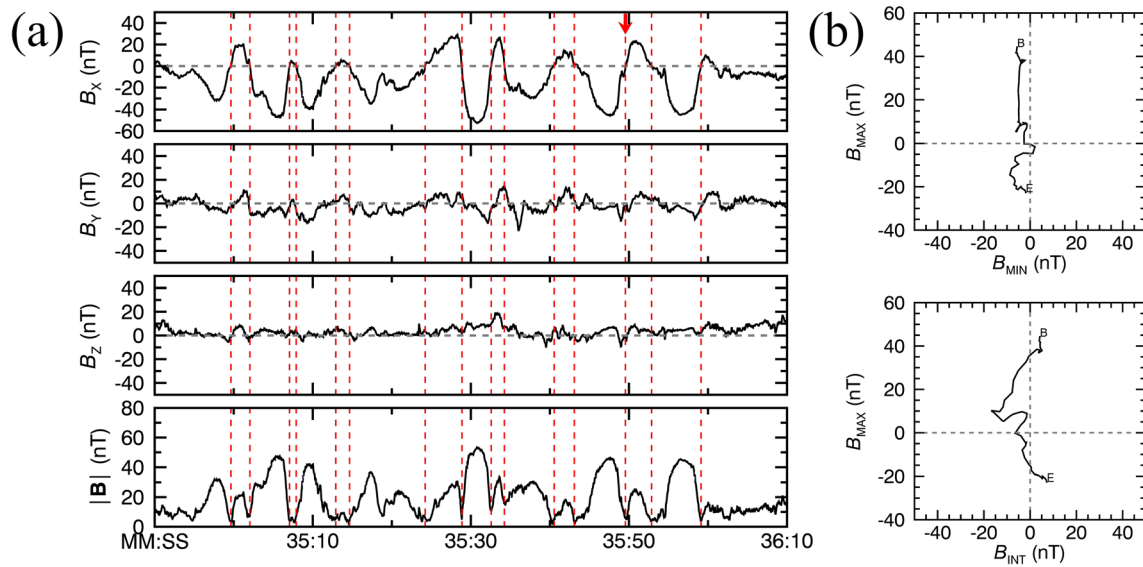


Figure 3. (a) Close-up interval of magnetic field measurements during encounter of Mercury’s cross-tail current sheet observed by MESSENGER on 19 May 2012 as shown in Figure 2. (b) MVA hodogram of a flapping wave example denoted by red arrow in (a).

components and magnitude of the observed magnetic field vectors. The interval starts with MESSENGER in the southern lobe of Mercury’s magnetotail characterized by the strong magnetic field predominantly in the negative B_x direction and low level of fluctuations in magnetic field. During this time period, MESSENGER observed a full (red dashed line) and several partial current sheet crossings (blue arrow). The former type of current sheet crossing is characterized by a positive-to-negative or negative-to-positive reversal of B_x , indicating that MESSENGER crosses the center of Mercury’s cross-tail current sheet. The latter is characterized by a decrease in the magnitude of B_x without a reversal in the sign of B_x , indicating that MESSENGER observed the flapping motion of the current sheet but did not cross its center (i.e., $B_x = 0$ nT).

At ~14:34:30 UTC, MESSENGER entered the cross-tail current sheet proper shown by the overall “slow” reversal of B_x from negative to positive, which is due to MESSENGER traversing through Mercury’s magnetotail. MESSENGER further observed frequent multiple large-amplitude B_x reversals of ~20–40 nT, superimposed on the overall slow reversal of B_x . Wavelet analysis of the B_x oscillations (panel 1) indicates that these flapping waves have a period of ~4–15 seconds. The half waveform of each B_x oscillation (i.e., a single flapping wave event) is identified with a red vertical dashed line. Since MESSENGER is deep in the cross-tail current sheet, only full current sheet crossings were observed in this time interval. As MESSENGER exited the cross-tail current sheet into the northern tail lobe, MESSENGER also observed seven partial crossing events (blue arrows) between 14:37 UTC and 14:39 UTC. Note that the partial flapping waves indicated by the blue arrows show a sharp minima and flat maxima in the absolute value of B_x . This type of waveform is consistent with the flapping current sheet scenario where the spacecraft is located north (or south) relative to the center of the flapping Harris current sheet. As the spacecraft moves away from the center of the current sheet, the gradient of B_x approaches zero, and when the spacecraft approaches the center of the current sheet, the gradient of B_x increases.

Figure 3a shows the 80-s-long interval between 14:35:50 UTC and 14:36:10 UTC of magnetic field measurements observed by MESSENGER in the same cross-tail current sheet encounter shown in Figure 2. Note that the time intervals with positive B_x shown in Figure 3 are systematically shorter than the time intervals with negative B_x and the absolute values of negative B_x are larger than that of positive B_x . These observed signatures are consistent with the scenario where the MESSENGER spacecraft traverses a sinusoidal current sheet (in the frame of the flapping wave) southward of the center of Mercury’s cross-tail current sheet. Furthermore, the gradient of B_x peaks at $B_x = 0$ nT, which is expected during the crossing of a Harris current sheet. These observations confirm that the variation in B_x is not random but the result of a sinusoidal flapping motion of the cross-tail current sheet.

Table 1
MVA Results for Flapping Wave Events Shown in Figure 2

	UTC (HH:MM:SS)	$\hat{\mathbf{n}}$	$\lambda_{\text{int}}/\lambda_{\text{min}}$	$\lambda_{\text{max}}/\lambda_{\text{int}}$	$\Delta\varphi_{\text{int,min}} (^{\circ})$	$\Delta\varphi_{\text{max,min}} (^{\circ})$
1	14:34:59	[0.07, -0.89, 0.44]	6.05	28.80	4.4	0.7
2	14:35:02	[-0.002, 0.57, 0.82]	4.53	28.40	10.9	1.6
3	14:35:07	[0.07, -0.45, 0.89]	8.27	49.88	5.1	0.6
4	14:35:08	[-0.16, 0.006, 0.99]	4.29	16.82	6.1	1.2
5	14:35:13	[-0.27, 0.43, 0.86]	2.52	47.21	7.0	0.6
6	14:35:14	[0.11, -0.09, 0.99]	2.64	13.47	7.0	1.2
7	14:35:24	[-0.17, 0.50, 0.85]	1.21	40.22	32.3	0.9
8	14:35:28	[-0.11, 0.73, 0.67]	1.97	139.42	17.3	0.7
9	14:35:32	[-0.004, -0.51, 0.86]	2.22	81.50	11.8	0.7
10	14:35:34	[-0.22, 0.15, 0.96]	3.20	23.67	9.3	1.3
11	14:35:40	[-0.28, 0.96, 0.03]	2.43	14.30	7.3	1.2
12	14:35:43	[0.03, -0.19, 0.98]	5.91	5.38	3.8	1.4
13	14:35:49	[0.01, -0.76, 0.65]	8.36	11.68	3.2	0.8
14	14:35:53	[-0.003, 0.09, 0.99]	2.23	67.26	6.9	0.5
15	14:35:59	[0.18, -0.70, 0.69]	14.13	46.26	3.0	0.4

Note. (Column 3) Current sheet normal \mathbf{n} computed from the MVA technique. (Columns 4 and 5) The intermediate-to-minimum and maximum-to-intermediate eigenvalues ratios. (Columns 6 and 7) The angular uncertainties of the minimum eigenvector for rotation toward or away from the intermediate and maximum eigenvectors (i.e., angular uncertainty cone around the current sheet normal vector), respectively.

For each flapping wave event identified visually, we performed the MVA (Sonnerup & Scheible, 1998) to determine the current sheet normal \mathbf{n} . Figure 3b shows the hodograms of the MVA result of a flapping wave example identified in Figure 3a at ~14:35:49 UTC (red arrow). The hodograms show a clear rotation in B_{max} with some and no variation in B_{int} and B_{min} , respectively, signatures typically representative of a CS crossing (Sonnerup & Scheible, 1998). The minimum \mathbf{v}_{min} (i.e., current sheet normal \mathbf{n}), intermediate \mathbf{v}_{int} , and maximum \mathbf{v}_{max} eigenvectors are [-0.01, -0.76, 0.65], [0.03, -0.65, -0.76], and [0.99, 0.03, 0.01]. We calculated the int-min and max-int eigenvalue ratios to be ~8.36 and 11.68, respectively. Using the error estimation method outlined in Khrabrov and Sonnerup (1998), we also computed the angular uncertainty $|\Delta\varphi|$ of the minimum eigenvectors for rotation toward or away from the intermediate and maximum eigenvectors (i.e., angular uncertainty cone around the current sheet normal vector) to be ~3.2° and 0.8°, respectively. Recent flapping wave studies (e.g., DiBraccio et al., 2017) use an eigenvalue ratio threshold of 3 to establish acceptability of MVA results. The large eigenvalue ratios (i.e., greater than 3) and the small calculated angular uncertainty cone indicate that the current sheet normal for this flapping wave example is well defined. It is interesting to note that \mathbf{n} (or \mathbf{v}_{min}) is tilted in the y - z plane as shown by the significantly larger values of n_y and n_z as compared to n_x , which is consistent with flapping waves observed at Earth and other planets (e.g., Volwerk et al., 2013, and references therein).

Table 1 shows the current sheet normal vectors with their associated angular uncertainties and eigenvalue ratios determined from MVA for all flapping waves events identified in this interval. Similar to the previous flapping wave example, the majority of the current sheet normal vectors \mathbf{n} of all flapping wave events within the interval have minor component in the x direction with significant components in either y or z direction or both, indicating that these cross-tail current sheets are tilted in the y - z plane. Our results also show a general pattern of most current sheet normal vectors “oscillating” in the y - z plane, where the y component of \mathbf{n} alternates in polarity between adjacent crossings. These observations are consistent with the encounter of a sinusoidal (or kink-type) flapping current sheet traveling in the cross-tail direction (e.g., Volwerk et al., 2013, and references therein). Note that it is unclear whether the flapping waves are traveling away from or toward the magnetotail flanks since we are unable to determine the actual direction of propagation with single-spacecraft measurements.

The error analysis of the MVA results also shows that the majority of the current sheet normally computed are generally reliable as reflected by the small angular uncertainty of the minimum eigenvector and/or the int-min eigenvalue ratios greater than 3, with the exception of few events (e.g., Event 7), which have large uncertainty angle cones due to their small int-min eigenvalue ratios. However, it is not surprising to

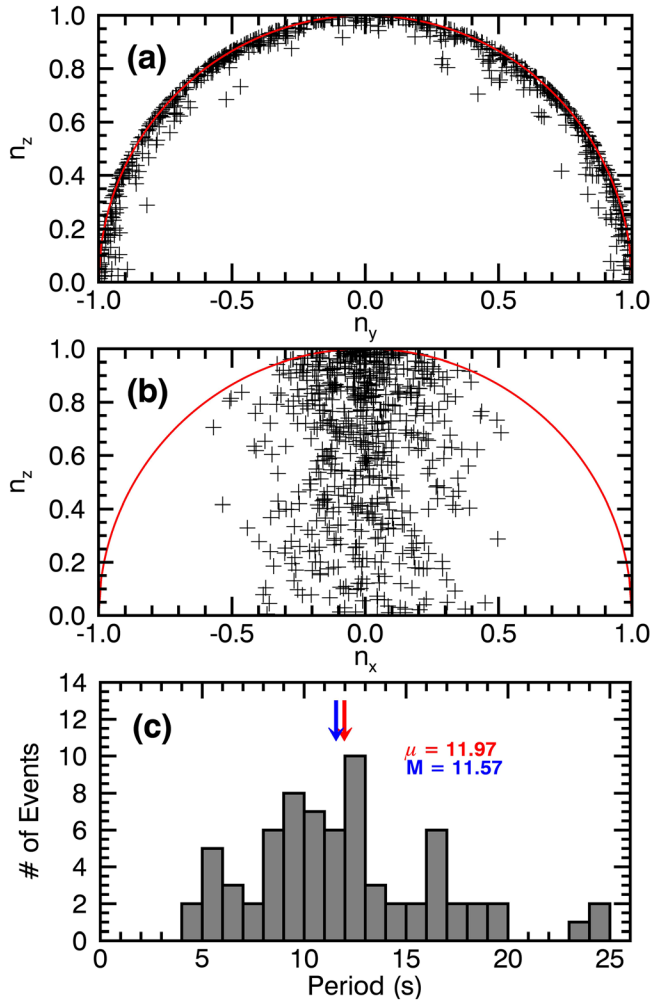


Figure 4. Distribution of current sheet normal vectors in (a) y - z and (b) x - z planes. The red line represents the $\sqrt{n_z^2 + n_y^2} = 1$ and $\sqrt{n_z^2 + n_x^2} = 1$ curves, respectively. (c) Distribution of the periods of flapping waves. μ and M in (c) represent the mean and median of the flapping wave periods, respectively.

observe MVA results with low int-min eigenvalue ratios for Mercury's cross-tail current sheet, which can be generally described by a Harris current sheet model (Poh et al., 2017a, 2017b). A small int-min eigenvalue ratio is generally expected of a Harris current sheet, which has a direction of maximum variance only (Forsyth et al., 2009). An accurate estimate of the normal using MVA technique can be obtained with sufficient measurements when there is sufficient deviation from the Harris model (i.e., presence of magnetic field component in the cross-tail direction or a magnetic shear). Therefore, only flapping wave events with int-min eigenvalue ratio greater than 3 will be used for subsequent statistical analysis. Despite the limitations of using the MVA technique to determine the cross-tail current sheet normal with single-spacecraft measurements, it is evident that the results from the MVA technique have captured the general behavior of the flapping motion of Mercury's cross-tail current sheet reasonably well.

2.2. Statistical Analysis

We surveyed 4 years of MESSENGER magnetic field data and visually identified 65 magnetotail encounters where large-amplitude, quasi-periodic magnetic field oscillations associated with flapping motion of Mercury's cross-tail current sheet were observed. In each magnetotail encounter with large-amplitude magnetic field oscillations, the characteristic B_x reversal signatures associated with the encounter of flapping waves were visually identified to distinguish between intervals with flapping waves and random magnetic field fluctuations or electromagnetic waves (Boardsen et al., 2012). MVA technique was then performed on each flapping wave event to determine the vector normal to the current sheet. Every MVA result was also visually inspected to ensure that the selected events are not associated with other magnetic structures (e.g., flux ropes, DiBraccio, Slavin, Imber, et al., 2015; dipolarization fronts, Dewey et al., 2017, 2018; Sundberg, Slavin, et al., 2012; Sun et al., 2016) observed in Mercury's magnetotail. A total of 638 flapping wave events was selected for further analysis.

Figures 4a and 4b show the distribution of the current sheet normal vectors in the y - z and x - z planes, respectively. Figure 4a shows that the current sheet normal vectors \mathbf{n} are distributed near the unit circle in the y - z plane (i.e., $\sqrt{n_z^2 + n_y^2} = 1$), while the vectors were distributed around $n_x = 0$ in the x - z plane as shown in Figure 4b. Our result strongly indicates that $|n_x| \ll |n_y|, |n_z|$, which means that the current sheet associated with these flapping motions is predominantly tilted (or warped) in the y - z direction. This characteristic y - z tilt in the current sheet associated with flapping waves observed at Mercury is similar to those observed at Earth from Geotail measurements (Sergeev et al., 2006), where the distribution of MVA normal in the y - z plane indicates a "yz-kink" type of flapping waves. Assuming that the flapping waves are planar structures, if the flapping waves were traveling in the downtail ($\pm x$) or cross-tail ($\pm y$) direction, one would expect the warping of the current sheet normal to be in the x - z or y - z planes, respectively. Hence, within the limits of single-spacecraft measurements, our results suggest that these flapping waves are likely to be traveling in the cross-tail direction with the orientation of the current sheet normal similar to that observed at Earth (Sergeev et al., 2006) and the giant planets (Volwerk et al., 2013).

We calculated the typical periods of the flapping waves from the results of the wavelet analysis. Figure 4c shows the distribution of flapping wave periods of all identified peaks in wave power associated with groups of flapping wave events. The distribution in Figure 4c shows a large range of flapping wave period of ~ 4 –25 seconds, and the average flapping wave period (oscillation frequency) is ~ 12 seconds (0.52 rad/s),

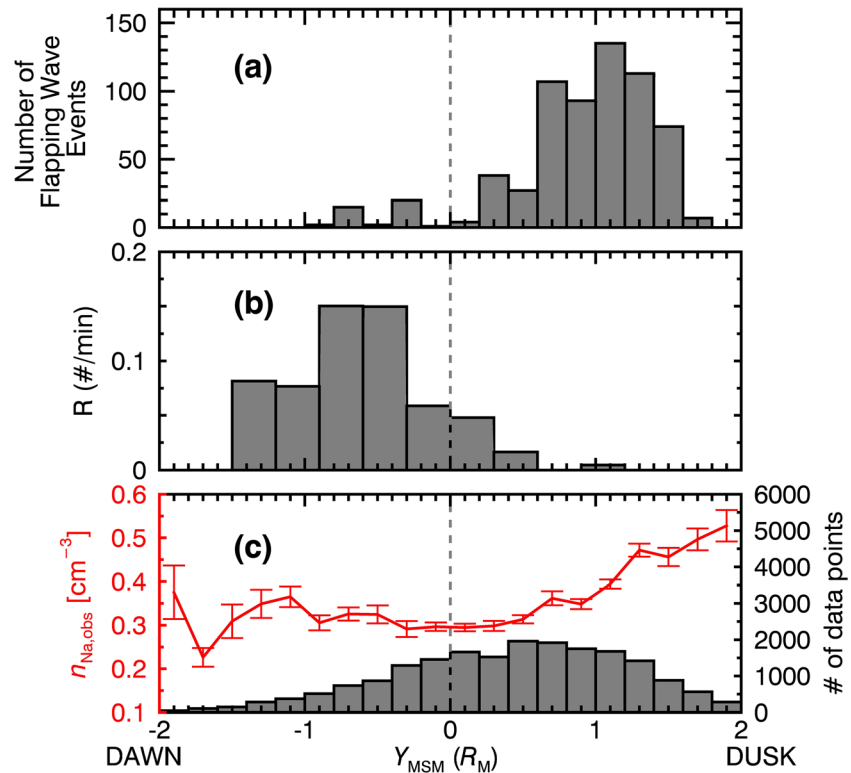


Figure 5. Dawn-dusk distribution of (a) flapping wave occurrences (bin size of $0.1 R_M$), (b) occurrence rate of dipolarization fronts (bin size of $0.3 R_M$) observed by MESSENGER (Sun et al., 2016), and (c) observed Na^+ density (bin size of $0.1 R_M$) in the cross-tail current sheet (i.e., $-1.5 > X_{MSM} (R_M) > -3.5$ and $0.4 > Z_{MSM} (R_M) > -0.4$). The dashed line represents the noon-midnight meridian (i.e., $Y_{MSM} = 0$). The error bars and histogram in (c) represent the standard error of the mean of the observed Na^+ density in each bin and the total number of data points in each bin, respectively.

which is much smaller than that observed at Earth and the outer planets (~ 2 – 10 minutes, Kubyshkina et al., 2014; Volwerk et al., 2013). Such significant difference in flapping period can be attributed to Mercury's smaller scale and more dynamic magnetosphere, and extreme solar wind conditions in the inner heliosphere (e.g., Jia et al., 2019; Slavin et al., 2014, 2019).

We also examined whether there is any dawn-dusk asymmetry in the occurrence of flapping waves at Mercury. Figure 5a shows the distribution of flapping wave occurrences as a function of Y_{MSM} . Interestingly, there is a strong duskward preference of the flapping wave events identified in this study in Mercury's cross-tail current sheet with peak occurrence at $Y_{MSM} \sim 1 R_E$. Note that this observed strong asymmetry is unlikely due to orbital selection bias during the survey of MESSENGER data as the spacecraft orbital trajectory precesses around Mercury's rotation axis, resulting in even local time coverage over one full precession. This dawn-dusk asymmetry in the occurrence of current sheet flapping waves is unique to Mercury since such asymmetry has not been observed in other planets. Possible relationships between the known asymmetries of Mercury's magnetotail and the observed duskward preference of flapping wave occurrence, and its implication on the excitation mechanism of Mercury's current sheet flapping waves will be further examined in section 3.

3. Discussion

Our analysis of Mercury's flapping waves shows that Mercury's cross-tail current sheet oscillates with period of ~ 4 – 25 seconds and that this flapping motion of the current sheet caused it to warp and become tilted in the y - z plane. This tilted current sheet geometry is similar to that of the flapping waves observed at Earth and is consistent with the scenario where the flapping waves are propagating in the cross-tail direction. Since we

cannot accurately determine the actual flapping wave propagation direction using single-spacecraft measurements, it is possible that these oscillatory motions of Mercury's current sheet are driven by an internal process within the magnetotail and/or external solar wind-driven processes. The natural follow-up question would be: What is the most plausible internal and/or external formation process or mechanism for Mercury's flapping waves?

3.1. Ballooning-Type Flapping Wave Model

Multiple models had been proposed to explain the formation and observations of flapping waves via an internal process at Earth. The ballooning-type (Golovchanskaya & Maltsev, 2005) and magnetic double-gradient instability models (Erkaev et al., 2007) are widely accepted internal flapping wave formation models. The ballooning-type model, similar to the interchange instability with magnetic tension on curved field lines serving the same role as gravitational force, requires the scale of the wavelength to be much smaller than the radius of curvature of the field lines (R_C) (Pritchett & Coroniti, 2010). In the midtail region (i.e., $-1.8 R_M > X_{MSM} > -3.8 R_M$) of Mercury's duskside current sheet where most flapping waves were observed, $R_C \sim 200$ km (Rong et al., 2018). We further assumed the characteristic wavelength of these flapping waves to be on the order of or larger than Mercury's cross-tail current sheet thickness ($\sim 0.4 R_M$ or ~ 976 km, Poh et al., 2017a). This is a valid assumption since the typical wavelength of flapping waves observed at Earth is several R_E (Runov et al., 2005; Sergeev et al., 2003; Wang et al., 2019), which is an order of magnitude larger than the average terrestrial cross-tail current sheet thickness during substorm conditions ($\sim 0.1 R_E$, Sergeev et al., 1990). Since the wavelength of the flapping waves is much larger than R_C of Mercury's duskside cross-tail current sheet, it is unlikely that the flapping waves observed at Mercury are caused by the ballooning-type instability.

3.2. Magnetic Double-Gradient Instability Flapping Wave Model

The magnetic double-gradient instability can occur when there is a "tailward B_Z gradient" magnetic field topology in the cross-tail current sheet, resulting in the unstable perturbation of the current sheet due to the force imbalance between the magnetic stress and total pressure gradient force in the quiescent current sheet along the z direction (see Figure 4 in Erkaev et al., 2008, for illustration). This perturbation of the current sheet drives the flapping waves in the cross-tail direction. Although both kink and sausage mode waves can be excited by this instability, Erkaev et al. (2008) demonstrated that the kink mode waves are more likely to be observed since it has a faster growth rate than the sausage mode. The characteristic oscillation frequency ω_f of the current sheet (Erkaev et al., 2008, 2010; Forsyth et al., 2009) depends on the product of the spatial gradients of B_X and B_Z and is given by the equation:

$$\omega_f = \sqrt{\frac{1}{\mu_0 m_p n_0} \left\langle \frac{\partial B_X}{\partial z} \right\rangle \frac{\partial B_Z}{\partial x} \Big|_{z=z_0}}, \quad (1)$$

where n_0 is the plasma density and $\frac{\partial B_X}{\partial z}$ and $\frac{\partial B_Z}{\partial x}$ are the spatial gradients of B_X and B_Z at the center of the cross-tail current sheet ($z = z_0$), respectively.

This "tailward B_Z gradient" (or $\frac{\partial B_Z}{\partial x} < 0$) magnetic field topology can be caused by the local thinning of the cross-tail current sheet in the near-tail region (Erkaev et al., 2008). The follow-up question is: How strong should the tailward B_Z gradient, if it exists, be for the double-gradient instability to create the observed quasi-periods of Mercury's flapping waves?

As a first-order approximation, we calculated $\frac{\partial B_X}{\partial z} \Big|_{z=z_0} \sim 165$ nT $-(R_M)^{-1}$ by differentiating the Harris current sheet equation at $z = z_0$, with the asymptotic lobe field B_0 and duskside current sheet half-thickness Δ to be ~ 41.4 nT and $0.25 R_M$, respectively (Poh et al., 2017a). Assuming $n_0 \sim 1$ cm $^{-3}$ for Mercury's central plasma sheet (Gershman et al., 2014; Poh et al., 2018; Raines et al., 2012) and $\langle \omega_f \rangle \sim 0.52$ rad/s determined from the wavelet analysis, we calculated the value of $\frac{\partial B_Z}{\partial x} \Big|_{z=z_0}$ required to create the observed current sheet oscillations to be ~ 19.52 nT/ R_M (~ 0.008 nT/km). Taking into consideration Hall effects in the double-gradient instability model (Erkaev et al., 2010), we further calculated the characteristic oscillation speed V_f (i.e.,

$\omega_p \Delta$) to be ~ 317 km/s and the dimensionless Hall parameter α (i.e., ratio of proton current speed to the characteristic oscillation speed) to be ~ 0.4 (Erkaev et al., 2010). We then determined the flapping wave group velocity V_g to be $\sim 0.5 V_f = 158$ km/s using the Hall parameter α of 0.4 solid curve in Figure 2a of Erkaev et al. (2010). It is worth noting that the calculated propagating velocity of Mercury's flapping waves is closer to the upper limit of the flapping waves observed at Earth, which ranges from few tens (Runov et al., 2005; Sun et al., 2014) to hundreds of km/s (Sergeev et al., 2006).

Our calculated gradient is approximately 2 orders of magnitude larger than that of Earth's ($\sim 6 \times 10^{-5}$ nT/km) (Erkaev et al., 2007), raising the question of whether such tailward B_z gradient configuration is possible in Mercury's magnetotail. Simulations (Hsieh & Otto, 2015) and observation (Sun, Fu, et al., 2017) at Earth have shown that magnetic flux depletion may occur in the Earth's near-tail region due to the azimuthal transport of closed magnetic flux from nightside to dayside along contours of constant flux tube entropy, resulting in current sheet thinning in the near-tail region. This process could make the B_z gradients in the cross-tail current sheet necessary to drive these kink-type current sheet oscillations at Mercury and should be further investigated in future simulation and observation studies.

3.3. External Excitation Mechanisms of Flapping Waves

The excitation of current sheet flapping waves inside planetary magnetotails due to solar wind variations as external driving mechanisms has also been explored from observational and modeling perspectives. Solar wind pressure perturbation-initiated motion of the cross-tail current sheet has been observed by McComas et al. (1986), Shen et al. (2008), and, more recently, Wang et al. (2019). The numerical model by Sergeev et al. (2008) showed that the total pressure difference between the north and south tail lobes caused by a solar wind directional discontinuity can result in vertical motion of the neutral sheet initiated at the tail center. Juusola et al. (2018) further demonstrated in their hybrid-Vlasov model that a north-south asymmetric magnetopause perturbation can displace the initial current and launch a standing magnetosonic wave within the tail resonance cavity. Both models suggest that the displacement of the neutral sheet by solar wind drivers can excite kink-like waves propagating from the tail center toward the flanks. Earlier Mercury studies on reconnection dynamics (e.g., DiBraccio et al., 2013; Slavin et al., 2014) show that the extreme low- β , high-dynamic-pressure solar wind conditions at Mercury drive intense reconnection and flux transfer generation at Mercury's magnetopause and, consequently, in the magnetotail. It is plausible that external solar wind drivers play an important role in exciting flapping waves within Mercury's magnetotail. However, in the absence of an upstream solar wind monitor, the question of the relationship between flapping waves' occurrence and solar wind perturbations as an external driving source can only be resolved through theory and numerical modeling.

3.4. Dawn-Dusk Asymmetric Distribution of Flapping Waves

Our statistical results also show that flapping waves are predominantly observed in Mercury's duskside cross-tail current sheet with peak occurrence at $Y_{\text{MSM}} \sim 1 R_M$. At Earth, the peak occurrence of flapping waves was observed near the tail center (Sergeev et al., 2006), which suggests that the source of flapping waves at Earth is located near the tail center. Following similar arguments to those used at Earth, this distinct preferred occurrence of Mercury's flapping waves observed at $Y_{\text{MSM}} \sim 1 R_M$ implies a duskward shift in the internal source of flapping waves as compared to Earth. Recent studies have revealed many asymmetries in Mercury's cross-tail current sheet properties (Poh et al., 2017b) and occurrence of reconnection-related phenomena. In particular, there is a dawnward preference in the occurrence of dipolarization fronts, often associated with high-speed flows, in Mercury's cross-tail current sheet (Dewey et al., 2018; Sun et al., 2016; Sun, Raines, et al., 2017) as shown in Figure 5b. At Earth, studies (Erkaev et al., 2009a, 2009b) have suggested a relationship between the occurrence of bursty bulk flows (BBFs) and flapping waves, where a fast moving flow burst from a reconnection region could excite kink-like perturbations in the current sheet away from the source. However, similar processes are not applicable to Mercury since both the occurrence of dipolarization fronts and flapping waves have opposite asymmetry. On the other hand, earlier studies (Liljeblad et al., 2015; Sundberg, Boardsen, et al., 2012) have shown a duskward preference in the occurrence of Kelvin-Helmholtz (K-H) waves at Mercury's magnetopause, which is similar to that of the flapping waves. This similarity in asymmetric occurrence indicates that K-H waves could be another possible external-source mechanism in exciting flapping motions of

Mercury's cross-tail current sheet. To date, there have not been any studies exploring the relationship between current sheet flapping waves and the occurrence of K-H waves as an external flapping source.

Interestingly, the observed dawn-dusk asymmetric distribution of current sheet flapping wave occurrence in Mercury's cross-tail current sheet is also similar to the spatial distribution of sodium ion (Na^+) density as shown in Figures 5a and 5c. Previous MESSENGER studies using the Fast Imaging Plasma Spectrometer (FIPS) instrument (Raines et al., 2013; Gershman et al., 2014) reported higher observed Na^+ density in the premidnight (or duskside) region of Mercury's plasma sheet, and this dawn-dusk Na^+ density asymmetry has also been observed in simulations (e.g., Chen et al., 2019; Yagi et al., 2017). Such dawn-dusk asymmetry in Na^+ density has been associated with the Na^+ dynamics in Mercury's magnetosphere, such as escape of Na^+ from a high-energy partial sodium ring during high solar wind dynamic pressure condition (Yagi et al., 2010, 2017) or centrifugal acceleration and transport of cold Na^+ from Mercury's cusp into the duskside plasma sheet via nonadiabatic Speiser-type orbits (Delcourt, 2013). It is possible that ion-ion hybrid resonance instability in a multispecies plasma sheet (i.e., proton and Na^+) (e.g., Buchsbaum, 1960) can drive fast magnetosonic waves propagating perpendicular to the magnetic field from the magnetopause toward the center of the cross-tail current sheet. These magnetosonic waves can then create localized spatial gradients in the magnetic field near the current sheet at scale lengths on the order of the Na^+ gyroradius, making the duskside cross-tail current sheet unstable to double-gradient instability. Although the flapping wave excitation mechanism described above is just as speculative as the other processes discussed in this study, it adequately explained the dawn-dusk asymmetry of the current sheet flapping wave occurrences.

From the above discussion, the excitation mechanism and duskward preference of flapping waves' occurrence at Mercury remain an open question. Future simulations (e.g., multifluid magnetohydrodynamic [MHD] and/or MHD with embedded particle-in-cell models) and theoretical studies should be conducted to further explore each possibility examined in this study to better our understanding of the excitation mechanism of flapping waves at Mercury and its unique observed dawn-dusk asymmetry.

4. Conclusion

In summary, we analyzed 638 flapping wave events identified from 65 MESSENGER crossings of Mercury's magnetotail. Our results can be summarized as follows:

1. Frequent large-amplitude oscillations of Mercury's cross-tail current sheet characterized by multiple B_x reversals with an average period of ~ 12 seconds were observed.
2. We determined that the flapping motion of Mercury's cross-tail current sheet warped and tilted the current sheet in the y - z plane.
3. The flapping waves preferentially occur on Mercury's duskside current sheet, which is similar to the dawn-dusk asymmetry pattern of the Na^+ density in Mercury's plasma sheet and K-H waves on Mercury's magnetopause.
4. The magnetic double-gradient instability is a plausible excitation mechanism for flapping wave formation at Mercury. However, other external (e.g., solar wind variations and K-H waves) and internal (e.g., finite gyroradius effects of planetary Na^+ on magnetosonic waves) processes are also possible excitation mechanisms for flapping wave formation at Mercury.

Acknowledgments

The authors acknowledged the support provided by the National Aeronautics and Space Administration (NASA) Discovery Data Analysis Program (DDAP) Grants NNX15K88G, NNX15AL01G, and NNX16AJ05G, Heliophysics Supporting Research (HSR) NNX15AJ68G, Living with a Star NNX16AJ67G, and Solar System Workings (SSW) Program Grant NNX15AH28G to the University of Michigan. The authors thank Dr. Martin Volwerk and the anonymous second reviewer for their helpful suggestions and reviews of this manuscript.

Data Availability Statement

Data sets analyzed in this study are archived with the NASA Planetary Data System (PDS) (<https://pds-ppi.igpp.ucla.edu/mission/MESSENGER>). The MAG CDR files in the PDS were used in this study.

References

- Anderson, B. J., Acuña, M. H., Lohr, D. A., Scheifele, J., Raval, A., Korth, H., & Slavin, J. A. (2007). The Magnetometer instrument on MESSENGER. *Space Science Reviews*, 131(1–4), 417–450. <https://doi.org/10.1007/s11214-007-9246-7>
- Anderson, B. J., Johnson, C. L., Korth, H., Purucker, M. E., Winslow, R. M., Slavin, J. A., et al. (2011). The global magnetic field of Mercury from MESSENGER orbital observations. *Science*, 333(6051), 1859–1862. <https://doi.org/10.1126/science.1211001>
- Boardsen, S. A., Slavin, J. A., Anderson, B. J., Korth, H., Schriver, D., & Solomon, S. C. (2012). Survey of coherent ~ 1 Hz waves in Mercury's inner magnetosphere from MESSENGER observations. *Journal of Geophysical Research*, 117, A00M05. <https://doi.org/10.1029/2012JA017822>

- Buchsbaum, S. J. (1960). Resonance in a plasma with two ion species. *The Physics of Fluids*, 3(3), 418–420. <https://doi.org/10.1063/1.1706052>
- Chen, Y., Tóth, G., Jia, X., Slavin, J. A., Sun, W., Markidis, S., et al. (2019). Studying dawn-dusk asymmetries of Mercury's magnetotail using MHD-EPIC simulations. *Journal of Geophysical Research: Space Physics*, 124, 8954–8973. <https://doi.org/10.1029/2019JA026840>
- Davey, E. A., Lester, M., Milan, S. E., & Fear, R. C. (2012). Storm and substorm effects on magnetotail current sheet motion. *Journal of Geophysical Research*, 117, A02202. <https://doi.org/10.1029/2011JA017112>
- Delcourt, D. C. (2013). On the supply of heavy planetary material to the magnetotail of Mercury. *Annales Geophysicae*, 31, 163–1679.
- Dewey, R. M., Raines, J. M., Sun, W., Slavin, J. A., & Poh, G. (2018). MESSENGER observations of fast plasma flows in Mercury's magnetotail. *Geophysical Research Letters*, 45, 10,110–10,118. <https://doi.org/10.1029/2018GL079056>
- Dewey, R. M., Slavin, J. A., Raines, J. M., Baker, D. N., & Lawrence, D. J. (2017). Energetic electron acceleration and injection during dipolarization events in Mercury's magnetotail. *Journal of Geophysical Research: Space Physics*, 122, 12,170–12,188. <https://doi.org/10.1002/2017JA024617>
- DiBraccio, G. A., Dann, J., Easley, J. R., Gruesbeck, J. R., Soobiah, Y., Connerney, J. E. P., et al. (2017). MAVEN observations of tail current sheet flapping at Mars. *Journal of Geophysical Research: Space Physics*, 122, 4308–4324. <https://doi.org/10.1002/2016JA023488>
- DiBraccio, G. A., Slavin, J. A., Boardsen, S. A., Anderson, B. J., Korth, H., Zurbuchen, T. H., et al. (2013). MESSENGER observations of magnetopause structure and dynamics at Mercury. *Journal of Geophysical Research: Space Physics*, 118, 997–1008. <https://doi.org/10.1002/jgra.50123>
- DiBraccio, G. A., Slavin, J. A., Imber, S. M., Gershman, D. J., Raines, J. M., Jackman, C. M., et al. (2015). MESSENGER observations of flux ropes in Mercury's magnetotail. *Planetary and Space Science*, 115, 77–89. <https://doi.org/10.1016/j.pss.2014.12.016>
- DiBraccio, G. A., Slavin, J. A., Raines, J. M., Gershman, D. J., Tracy, P. J., Boardsen, S. A., et al. (2015). First observations of Mercury's plasma mantle by MESSENGER. *Geophysical Research Letters*, 42, 9666–9675. <https://doi.org/10.1002/2015GL065805>
- Duan, A., Zhang, H., & Lu, H. (2018). 3D MHD simulation of the double-gradient instability of the magnetotail current sheet. *SCIENCE CHINA Technological Sciences*, 61(9), 1364–1371. <https://doi.org/10.1007/s11431-017-9158-7>
- Erkaev, N. V., Semenov, V. S., & Biernat, H. K. (2007). Magnetic double gradient instability and flapping waves in a current sheet. *Physical Review Letters*, 99(23), 235,003. <https://doi.org/10.1103/PhysRevLett.99.235003>
- Erkaev, N. V., Semenov, V. S., & Biernat, H. K. (2008). Magnetic double gradient mechanism for flapping oscillations of a current sheet. *Geophysical Research Letters*, 35, L02111. <https://doi.org/10.1029/2007GL032277>
- Erkaev, N. V., Semenov, V. S., & Biernat, H. K. (2010). Hall magnetohydrodynamic effects for current sheet flapping oscillations related to the magnetic double gradient mechanism. *Physics of Plasmas*, 17(6), 060703. <https://doi.org/10.1063/1.3439687>
- Erkaev, N. V., Semenov, V. S., Kubyshekin, I. V., Kubyshekina, M. V., & Biernat, H. K. (2009a). MHD aspect of current sheet oscillations related to magnetic field gradient. *Annales de Geophysique*, 27(1), 417–425. <https://doi.org/10.5194/angeo-27-417-2009>
- Erkaev, N. V., Semenov, V. S., Kubyshekin, I. V., Kubyshekina, M. V., & Biernat, H. K. (2009b). MHD model of the flapping motions in the magnetotail current sheet. *Journal of Geophysical Research*, 114, A03206. <https://doi.org/10.1029/2008JA013728>
- Forsyth, C., Lester, M., Fear, R. C., Lucek, E., Dandouras, I., Fazakerley, A. N., et al. (2009). Solar wind and substorm excitation of the wavy current sheet. *Annales de Geophysique*, 27(6), 2457–2474. <https://doi.org/10.5194/angeo-27-2457-2009>
- Gao, J. W., Rong, Z. J., Cai, Y. H., Lui, A. T. Y., Petrukovich, A. A., Shen, C., et al. (2018). The distribution of two flapping types of magnetotail current sheet: Implication for the flapping mechanism. *Journal of Geophysical Research: Space Physics*, 123, 7413–7423. <https://doi.org/10.1029/2018JA025695>
- Gershman, D. J., Slavin, J. A., Raines, J. M., Zurbuchen, T. H., Anderson, B. J., Korth, H., et al. (2014). Ion kinetic properties in Mercury's pre-midnight plasma sheet. *Geophysical Research Letters*, 41, 5740–5747. <https://doi.org/10.1002/2014GL060468>
- Golovchanskaya, I. V., & Maltsev, Y. P. (2005). On the identification of plasma sheet flapping waves observed by Cluster. *Geophysical Research Letters*, 32, L02102. <https://doi.org/10.1029/2004GL021552>
- Hsieh, M.-S., & Otto, A. (2015). Thin current sheet formation in response to the loading and the depletion of magnetic flux during the substorm growth phase. *Journal of Geophysical Research: Space Physics*, 120, 4264–4278. <https://doi.org/10.1002/2014JA020925>
- Jenkins, G. M., & Watts, D. G. (1968). *Spectral analysis and its applications*, (p. 525). Boca Raton, Fla: Holden-Day.
- Jia, X., Slavin, J. A., Poh, G., DiBraccio, G. A., Toth, G., Chen, Y., et al. (2019). MESSENGER observations and global simulations of highly compressed magnetosphere events at Mercury. *Journal of Geophysical Research: Space Physics*, 124, 229–247. <https://doi.org/10.1029/2018JA026166>
- Juusola, L., Pfau-Kempf, Y., Ganse, U., Battarbee, M., Brito, T., Grandin, M., et al. (2018). A possible source mechanism for magnetotail current sheet flapping. *Annales de Geophysique*, 36(4), 1027–1035. <https://doi.org/10.5194/angeo-36-1027-2018>
- Korovinskiy, D. B., Erkaev, N. V., Semenov, V. S., Ivanov, I. B., Kiehas, S. A., & Ryzhkov, I. I. (2018). On the influence of the local maxima of total pressure on the current sheet stability to the kink-like (flapping) mode. *Physics of Plasmas*, 25(2), 022904. <https://doi.org/10.1063/1.5016934>
- Korovinskiy, D. B., Ivanov, I. B., Semenov, V. S., Erkaev, N. V., & Kiehas, S. A. (2016). Numerical linearized MHD model of flapping oscillations. *Physics of Plasmas*, 23(6), 062905. <https://doi.org/10.1063/1.4954388>
- Khrabrov, A. V., & Sonnerup, B. U. (1998). Error estimates for minimum variance analysis. *Journal of Geophysical Research: Space Physics*, 103(A4), 6641–6651. <https://doi.org/10.1029/97JA03731>
- Kubyshekina, D. I., Sormakov, D. A., Sergeev, V. A., Semenov, V. S., Erkaev, N. V., Kubyshekin, I. V., et al. (2014). How to distinguish between kink and sausage modes in flapping oscillations? *Journal of Geophysical Research: Space Physics*, 119, 3002–3015. <https://doi.org/10.1002/2013JA019477>
- Liljeblad, E., Sundberg, T., Karlsson, T., & Kullen, A. (2015). Statistical investigation of Kelvin-Helmholtz waves at the magnetopause of Mercury. *Journal of Geophysical Research: Space Physics*, 119, 9670–9683. <https://doi.org/10.1002/2014JA020614>
- Liu, Y.-H., Li, T. C., Hesse, M., Sun, W.-J., Liu, J., Burch, J., et al. (2019). Three-dimensional magnetic reconnection with a spatially confined X-line extent: Implications for dipolarizing flux bundles and the dawn-dusk asymmetry. *Journal of Geophysical Research: Space Physics*, 124, 2819–2830. <https://doi.org/10.1029/2019JA026539>
- McComas, D. J., Russell, C. T., Elphic, R. C., & Bame, S. J. (1986). The near-Earth cross-tail current sheet: Detailed ISEE 1 and 2 case studies. *Journal of Geophysical Research*, 91(A4), 4287–4301. <https://doi.org/10.1029/JA091A04p04287>
- Poh, G., Slavin, J. A., Jia, X., Raines, J. M., Imber, S. M., Sun, W.-J., et al. (2017a). Mercury's cross-tail current sheet: Structure, X-line location and stress balance. *Geophysical Research Letters*, 44, 678–686. <https://doi.org/10.1002/2016GL071612>
- Poh, G., Slavin, J. A., Jia, X., Raines, J. M., Imber, S. M., Sun, W.-J., et al. (2017b). Coupling between Mercury and its nightside magnetosphere: Cross-tail current sheet asymmetry and substorm current wedge formation. *Journal of Geophysical Research: Space Physics*, 122, 8419–8433. <https://doi.org/10.1002/2017JA024266>

- Poh, G., Slavin, J. A., Jia, X., Sun, W.-J., Raines, J. M., Imber, S. M., et al. (2018). Transport of mass and energy in Mercury's plasma sheet. *Geophysical Research Letters*, *45*, 12,163–12,170. <https://doi.org/10.1029/2018GL080601>
- Pritchett, P. L., & Coroniti, F. V. (2010). A kinetic ballooning/interchange instability in the magnetotail. *Journal of Geophysical Research*, *115*, A06301. <https://doi.org/10.1029/2009JA014752>
- Raines, J. M., Gershman, D. J., Zurbuchen, T. H., Sarantos, M., Slavin, J. A., Gilbert, J. A., et al. (2012). Distribution and compositional variations of plasma ions in Mercury's space environment: The first three Mercury years of MESSENGER observations. *Journal of Geophysical Research*, *118*, 1604–1619. <https://doi.org/10.1029/2012JA018073>
- Raines, J. M., Slavin, J. A., Zurbuchen, T. H., Gloeckler, G., Anderson, B. J., Baker, D. N., et al. (2011). MESSENGER observations of the plasma environment near Mercury. *Planetary and Space Science*, *59*(15), 2004–2015. <https://doi.org/10.1016/j.pss.2011.02.004>
- Rong, Z. J., Barabash, S., Stenberg, G., Futaana, Y., Zhang, T. L., Wan, W. X., et al. (2015). Technique for diagnosing the flapping motion of magnetotail current sheets based on single-point magnetic field analysis. *Journal of Geophysical Research: Space Physics*, *120*, 3462–3474. <https://doi.org/10.1002/2014JA020973>
- Rong, Z. J., Ding, Y., Slavin, J. A., Zhong, J., Poh, G., Sun, W. J., et al. (2018). The magnetic field structure of Mercury's magnetotail. *Journal of Geophysical Research: Space Physics*, *123*, 548–566. <https://doi.org/10.1002/2017JA024923>
- Runov, A., Sergeev, V. A., Baumjohann, W., Nakamura, R., Apatenkov, S., Asano, Y., et al. (2005). Electric current and magnetic field geometry in flapping magnetotail current sheets. *Annales Geophysicae*, *23*(4), 1391–1403. <https://doi.org/10.5194/angeo-23-1391-2005>
- Sergeev, V., Angelopoulos, V., Carlson, C., & Sutcliffe, P. (1998). Current sheet measurements within a flapping plasma sheet. *Journal of Geophysical Research*, *103*(A5), 9177–9187. <https://doi.org/10.1029/97JA02093>
- Sergeev, V. A., Tanskanen, P., Mursula, K., Korth, A., & Elphic, R. C. (1990). Current sheet thickness in the near Earth plasma sheet during substorm growth phase. *Journal of Geophysical Research*, *95*(A4), 3819–3828. <https://doi.org/10.1029/JA095iA04p03819>
- Sergeev, V., Runov, A., Baumjohann, W., Nakamura, R., Zhang, T. L., Volwerk, M., et al. (2003). Current sheet flapping motion and structure observed by Cluster. *Geophysical Research Letters*, *30*(6), 1327. <https://doi.org/10.1029/2002GL016500>
- Sergeev, V., Sormakov, D. A., Apatenkov, S. V., Baumjohann, W., Nakamura, R., Runov, A. V., et al. (2006). Survey of large-amplitude flapping motions in the midtail current sheet. *Annales de Geophysique*, *24*(7), 2015–2024. <https://doi.org/10.5194/angeo-24-2015-2006>
- Sergeev, V. A., Tsyganenko, N. A., & Angelopoulos, V. (2008). Dynamical response of the magnetotail to changes of the solar wind direction: An MHD modeling perspective. *Annales de Geophysique*, *26*(8), 2395–2402. <https://doi.org/10.5194/angeo-26-2395-2008>
- Shen, C., Rong, Z. J., Li, X., Dunlop, M., Liu, Z. X., Malova, H. V., et al. (2008). Magnetic configurations of tail tilted current sheet. *Annales de Geophysique*, *26*(11), 3525–3543. <https://doi.org/10.5194/angeo-26-3525-2008>
- Slavin, J. A., Anderson, B. J., Baker, D. N., Benna, M., Boardsen, S. A., Gold, R. E., et al. (2012). MESSENGER and Mariner 10 flyby observations of magnetotail structure and dynamics at Mercury. *Journal of Geophysical Research*, *117*, A01215. <https://doi.org/10.1029/2011JA016900>
- Slavin, J. A., DiBraccio, G. A., Gershman, D. J., Imber, S. M., Poh, G. K., Raines, J. M., et al. (2014). MESSENGER observations of Mercury's dayside magnetosphere under extreme solar wind conditions. *Journal of Geophysical Research: Space Physics*, *119*, 8087–8116. <https://doi.org/10.1002/2014JA020319>
- Slavin, J. A., Middleton, H. R., Raines, J. M., Jia, X., Zhong, J., Sun, W.-J., et al. (2019). MESSENGER observations of disappearing dayside magnetosphere events at Mercury. *Journal of Geophysical Research: Space Physics*, *124*, 6613–6635. <https://doi.org/10.1029/2019JA026892>
- Sonnerup, B. U. Ö., & Scheible, M. (1998). Minimum and maximum variance analysis. In G. Paschmann, & P. Daly (Eds.), *Analysis methods for multi-spacecraft data*, (pp. 185–220). Noordwijk, Netherlands: Eur. Space Agency.
- Speiser, T. W., & Ness, N. F. (1967). The neutral sheet in the geomagnetic tail: Its motion, equivalent currents, and field line connection through it. *Journal of Geophysical Research*, *72*(1), 131–141. <https://doi.org/10.1029/JZ072i001p00131>
- Sun, W., Fu, S., Shi, Q., Zong, Q., Yao, Z., Xiao, T., & et al. (2014). THEMIS observation of a magnetotail current sheet flapping wave. *Chinese Science Bulletin*, *59*(2), 154–161. <https://doi.org/10.1007/s11434-013-0056-x>
- Sun, W.-J., Slavin, J. A., Fu, S., Raines, J. M., Sundberg, T., Zong, Q.-G., et al. (2015). MESSENGER observations of Alfvénic and compressional waves during Mercury's substorms. *Geophysical Research Letters*, *42*, 6189–6198. <https://doi.org/10.1002/2015GL065452>
- Sun, W. J., Fu, S. Y., Slavin, J. A., Raines, J. M., Zong, Q. G., Poh, G. K., & Zurbuchen, T. H. (2016). Spatial distribution of Mercury's flux ropes and reconnection fronts: MESSENGER observations. *Journal of Geophysical Research: Space Physics*, *121*, 7590–7607. <https://doi.org/10.1002/2016JA022787>
- Sun, W. J., Fu, S. Y., Wei, Y., Yao, Z. H., Rong, Z. J., Zhou, X. Z., et al. (2017). Plasma sheet pressure variations in the near-Earth magnetotail during substorm growth phase: THEMIS observations. *Journal of Geophysical Research: Space Physics*, *122*, 12,212–12,228. <https://doi.org/10.1002/2017JA024603>
- Sun, W. J., Raines, J. M., Fu, S. Y., Slavin, J. A., Wei, Y., Poh, G. K., et al. (2017). MESSENGER observations of the energization and heating of protons in the near-Mercury magnetotail. *Geophysical Research Letters*, *44*, 8149–8158. <https://doi.org/10.1002/2017GL074276>
- Sun, W. J., Shi, Q. Q., Fu, S. Y., Zong, Q. G., Pu, Z. Y., Xie, L., et al. (2010). Statistical research on the motion properties of the magnetotail current sheet: Cluster observations. *Science China Technological Sciences*, *53*(6), 1732–1738. <https://doi.org/10.1007/s11431-010-3153-y>
- Sun, W. J., Slavin, J. A., Dewey, R. M., Chen, Y., DiBraccio, G. A., Raines, J. M., et al. (2020). MESSENGER observations of Mercury's nightside magnetosphere under extreme solar wind conditions: Reconnection-generated structures and steady convection. *Journal of Geophysical Research: Space Physics*, *125*, e2019JA027490. <https://doi.org/10.1029/2019JA027490>
- Sundberg, T., Boardsen, S. A., Slavin, J. A., Anderson, B. J., Korth, H., Zurbuchen, T. H., et al. (2012). MESSENGER orbital observations of large-amplitude Kelvin-Helmholtz waves at Mercury's magnetopause. *Journal of Geophysical Research*, *117*, A04216. <https://doi.org/10.1029/2011JA017268>
- Sundberg, T., Slavin, J. A., Boardsen, S. A., Anderson, B. J., Korth, H., Ho, G. C., et al. (2012). MESSENGER observations of dipolarization events in Mercury's magnetotail. *Journal of Geophysical Research*, *117*, A00M03. <https://doi.org/10.1029/2012JA017756>
- Tsyganenko, N. A. (1995). Modeling the Earth's magnetospheric magnetic field confined within a realistic magnetopause. *Journal of Geophysical Research*, *100*(A4), 5599–5612. <https://doi.org/10.1029/94JA03193>
- Volwerk, M., André, N., Arridge, C. S., Jackman, C. M., Jia, X., Milan, S. E., et al. (2013). Comparative magnetotail flapping: An overview of selected events at Earth, Jupiter and Saturn. *Annales de Geophysique*, *31*(5), 817–833. <https://doi.org/10.5194/angeo-31-817-2013>
- Wang, G. Q., Zhang, T. L., Wu, M. Y., Schmid, D., Cao, J. B., & Volwerk, M. (2019). Solar wind directional change triggering flapping motions of the current sheet: MMS observations. *Geophysical Research Letters*, *46*, 64–70. <https://doi.org/10.1029/2018GL080023>
- Winslow, R. M., Anderson, B. J., Johnson, C. L., Slavin, J. A., Korth, H., Purucker, M. E., et al. (2013). Mercury's magnetopause and bow shock from MESSENGER Magnetometer observations. *Journal of Geophysical Research: Space Physics*, *118*, 22133. <https://doi.org/10.1002/jgra.50237>

- Yagi, M., Seki, K., Matsumoto, Y., Delcourt, D. C., & Leblanc, F. (2010). Formation of a sodium ring in Mercury's magnetosphere. *Journal of Geophysical Research*, *115*, A10253. <https://doi.org/10.1029/2009JA015226>
- Yagi, M., Seki, K., Matsumoto, Y., Delcourt, D. C., & Leblanc, F. (2017). Global structure and sodium ion dynamics in Mercury's magnetosphere with the offset dipole. *Journal of Geophysical Research: Space Physics*, *122*, 10,990–11,002. <https://doi.org/10.1002/2017JA024082>
- Zhang, T. L., Baumjohann, W., Nakamura, R., Balogh, A., & Glassmeier, K.-H. (2002). A wavy twisted neutral sheet observed by Cluster. *Geophysical Research Letters*, *29*(19), 1899. <https://doi.org/10.1029/2002GL015544>